JOURNAL OF GEOPHYSICAL RESEARCH, VOL. ???, NO. , PAGES 1–13,

A statistical model for the timing of earthquakes and volcanic eruptions influenced by periodic processes

Tim Jupp

BP Institute for Multiphase Flow, University of Cambridge, Cambridge, U.K.

David Pyle and Ben Mason

Department of Earth Sciences, University of Cambridge, Cambridge, U.K.

Brian Dade

Department of Earth Sciences, Dartmouth College, Hanover, New Hamphsire, U.S.A.

Abstract.

Evidence of non-uniformity in the rate of seismicity and volcanicity has been sought on a variety of timescales ranging from 12 hours (tidal) to $10^3 - 10^4$ years (climatic), but the results are mixed. Here, we propose a simple conceptual model for the influence of periodic processes on the frequency of geophysical 'failure events' such as earthquakes and volcanic eruptions. In our model a failure event occurs at a 'failure time' $t_F = t_I + t_R$ which is controlled by an 'initiation event' at the 'initiation time' t_I and by the 'response time' of the system t_R. We treat each of the initiation time, the response time and the failure time as random variables. In physical terms, we define the initiation time to be the time at which a 'load function' exceeds a 'strength function' and we imagine that the 'response time' t_R corresponds to a physical process such as crack propagation or the movement of magma.

Assuming that the magnitude and frequency of the periodic process are known, we calculate the statistical distribution of the initiation times on the assumption that the load and strength functions are otherwise linear in time. This allows the distribution of the failure times to be calculated, if the distribution of the response times is known also.

The predictions of this simple theory are compared with some examples of observed periodicity in seismic and volcanic activity at tidal and annual timescales.

1. Introduction

It has been suggested that time-periodic processes over a wide range of timescales may be responsible for the modulation of seismicity and volcanic activity. On a daily timescale, oceanic and earth tides have been been considered as possible triggers of seismicity [e.g. Wilcock, 2001; Vidale *et al.*, 1998] and volcanicity [e.g. Johnston and Mauk, 1972; Mauk and Johnston, 1973; Dzurisin, 1984]. Daily variations in temperature and atmospheric pressure have also been suggested as modulators of volcanic activity [e.g. Mastin, 1994; Neuberg, 2000]. On an annual timescale, barometric pressure [Gao *et al.*, 2000] and loading by snow [Heki, 2001] have been investigated along with annual changes in sea level [e.g. Mason *et al.*, 2002; McNutt and Beavan, 1987]. Finally, on a timescale of thousands of years, climatic changes in sea level and ice loading have been proposed as possible modulators of historical volcanic activity [e.g. Jull and McKenzie, 1996; McGuire *et al.*, 1997; Glazner *et al.*, 1999].

Our aim in this paper is to derive a simple statistical model of the times at which 'failure events' (such as earthquakes and volcanic eruptions) occur under the influence of a periodic process whose magnitude and period are known. We use an intuitively reasonable model for 'failure events' in which the failure process begins when a 'load function' first exceeds a 'strength function' as shown in Figure 1 [Lockner and Beeler, 1999].

Having derived the statistical distribution of the failure times we then discuss how this model might be applied to geophysical data. In particular, we discuss the contrasting evidence for non-uniformity in the global volcanic eruption rate at the annual timescale and at the tidal timescale. It appears that the volcanic eruption rate displays non-uniformity of up to 18% on an annual timescale but no significant periodicity has been found at the tidal timescale (12 hours) [Mason *et al.*, 2002].

Copyright 2003 by the American Geophysical Union.

Paper number .
0148-0227/03/$9.00

2. Outline of model

Our conceptual model is one in which an initiation event at time t_I marks the beginning of a failure process (such as crack propagation or the movement of magma) which causes a failure event (such as an earthquake or a volcanic eruption) to occur at a subsequent time t_F (Figure 1). The duration of the failure process is labelled the response time t_R and so the failure time is simply the sum of the initiation and response times: $t_F = t_I + t_R$. We suppose that an initiation event

occurs when a 'load' function $x_L(t)$ first exceeds a 'strength' function $x_S(t)$. It follows that the 'initiation time' t_I is the smallest value of t for which $x_L(t) = x_S(t)$. For example, the load function might represent the pressure of magma within a magma chamber (Figure 1a) or the shear stress across a geological fault (Figure 1b). Periodic variations in 'load' can therefore arise if periodic loading of the crust affects variables such as magma pressure or shear stress. Similarly, periodic variations in 'strength' can occur if faults are 'clamped' or 'unclamped' by changes in the normal stress across the fault [Stein, 1999] (Figure 1b). We emphasise that the load and strength functions $x_L(t)$ and $x_S(t)$ need not necessarily have the dimensions of stress. They could equally well represent strains or displacements. Our requirement is simply that the load and the strength have the same dimensions and that an 'initiation event' should occur at the point when the 'load' first exceeds the 'strength'.

Our ultimate aim in this paper is to derive an expression for the statistical distribution of the failure time $t_F = t_I + t_R$ when an external 'periodic process' imposes time-periodic variations on either the load or the strength. Our model is therefore a quantitative extension of those described qualitatively by Vidale *et al.* (1998) and Lockner and Beeler (1999). In this paper we seek to generalise these models by including the concept of a stochastic response time and by deriving analytical expressions for the statistical distributions of the initiation, response and failure times.

We suppose that the periodic process under consideration imposes a single sinusoidal perturbation of known amplitude A and known angular frequency ω on either the strength or the load. There are many periodic processes, operating over a wide range of timescales, which lead to perturbations of this sort. Examples include earth and ocean tides, annual changes in sea level and barometric pressure, and changes in crustal loading from snow and ice. For simplicity we suppose that in the absence of the periodic process the load and the strength approach each other linearly with time (Figure 2). This assumption is valid provided that the load and strength functions are approximately linear over the periodic timescale $1/\omega$. (In section 3.1 below we consider qualitatively the consequences of relaxing this requirement.)

We consider two classes of situation (Figure 2), which are mathematically equivalent. In the first case (Figure 2a), the load increases linearly with time while the periodic process imposes sinusoidal perturbations on an otherwise constant 'failure strength' x_0, giving the simple model

$$\text{model 1}: \begin{cases} x_L(t) &= m(t - t_T) \\ x_S(t) &= x_0 + A\sin\omega t \end{cases} \qquad (1)$$

where m is the linear rate of increase of the load and t_T is a time translation parameter controlling the time at which the load is taken to be zero. With the convention that $A > 0$,

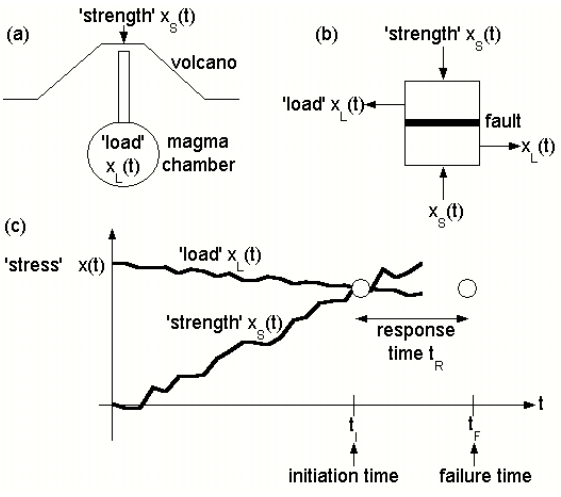

Figure 1. A conceptual overview of the model. (a) In the context of volcanic eruptions, we suppose that eruptions are initiated when the pressure of magma in a magma chamber (represented by $x_L(t)$) exceeds a critical 'strength' (represented by $x_S(t)$); (b) In the context of earthquakes, we suppose that movement on faults is initiated when the shear stress on the fault (represented by $x_L(t)$) exceeds the Coulomb failure stress [Stein, 1999] (represented by $x_S(t)$) which is related to the normal stress on the fault; (c) Volcanic and seismic events can both be viewed in terms of an initiation event at the initiation time t_I which occurs when the 'load function' $x_L(t)$ first exceeds the 'strength function' $x_S(t)$. After a subsequent response time t_R the system fails at the 'failure time' $t_F = t_I + t_R$.

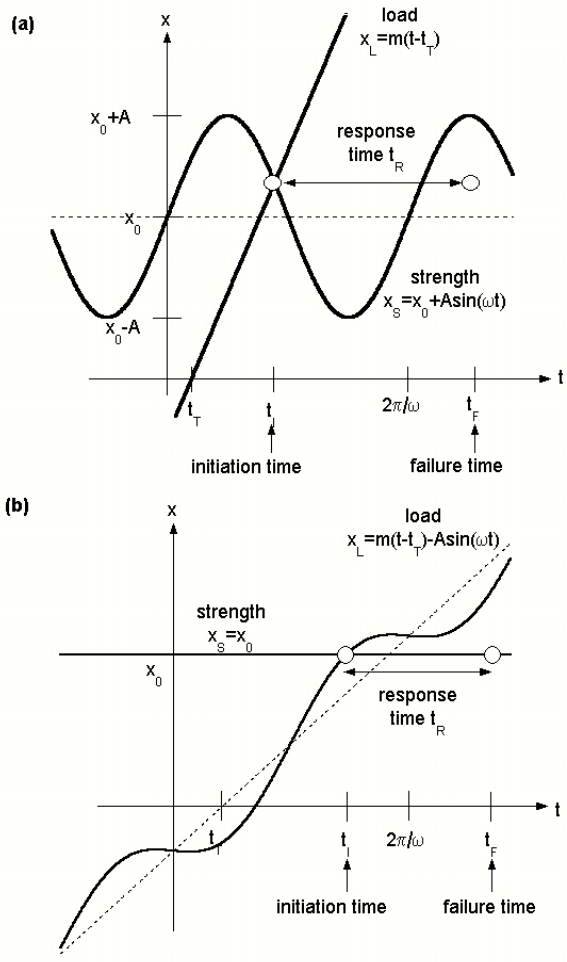

Figure 2. Sketches of the two types of process which are considered to lead to an initiation event. The two models are mathematically equivalent. (a) Model 1: The load increases linearly at rate m while the periodic process causes the strength to oscillate about a mean failure strength x_0; (b) Model 2: The strength is constant while the periodic process causes the load to oscillate about a linearly increasing trend of rate m.

Table 1. Representative parameter values for various periodic processes.

Process	Magnitude A (kPa)	Frequency ω (rad.s^{-1})	Rate $A\omega$ (Pa.s^{-1})
annual barometric[a]	1	$2 \cdot 10^{-7}$	$2 \cdot 10^{-4}$
semi-diurnal ocean tide[b]	10	$1.45 \cdot 10^{-4}$	1.45
annual sea level[c]	1	$2 \cdot 10^{-7}$	$2 \cdot 10^{-4}$
climatic sea level[d]	1000	$2 \cdot 10^{-11}$	$2 \cdot 10^{-5}$

[a] Adapted from Gao *et al.* (2000).

[b] Adapted from Wilcock (2001) assuming ocean tides of magnitude 1 m at the dominant tidal period 12.4 hours.

[c] Adapted from Mason *et al.* (2002) assuming an annual sealevel variation of 10 cm.

[d] Adapted from McGuire *et al.* (1997) assuming a sealevel change of 100 m in 10,000 years.

the origin of the time axis in equation 1 has been chosen so that the fluctuation in strength takes a maximum (positive) value when $\omega t = \pi/2$ (Figure 2*a*). Variation of the parameter t_T corresponds to translation of the load lines along the time axis and so influences the time at which the load and the strength intersect. In the context of earthquakes, a representative value of the linear rate m is given by the 'typical' rate of increase of tectonic stress $m \sim 10^{-4}$ bar.hr^{-1} (or $2.8 \cdot 10^{-3}$ Pa.s^{-1}) quoted by Vidale *et al.* (1998). In a volcanic context, measured rates of tectonic stress accumulation m at individual volcanoes have been reported in the range $2 \cdot 10^{-2}$ Pa.s^{-1} to 80 Pa.s^{-1} [Mauk and Johnston, 1973; Sparks 1981]. Similarly, 'typical' values of the magnitude A and angular frequency ω of various periodic processes are given in Table 1.

In the second case (Figure 2*b*), we suppose that the periodic process affects the load rather than the strength. Physical examples of this situation include the changes in shear stress across a geological fault [Perfettini and Schmittbuhl, 2001] (Figure 1*b*) and variations in the pressure of magma within a magma chamber (Figure 1*a*). In this case the load consists of sinusoidal perturbations about an upward linear trend of rate m while the strength remains constant. This gives the model

$$\text{model 2}: \begin{cases} x_L(t) &= m(t - t_T) - A \sin \omega t \\ x_S(t) &= x_0 \end{cases} \qquad (2)$$

which is analogous to equation 1. Assuming again that $A > 0$, the origin of the time axis has been chosen in such a way that the fluctuation in load takes a maximum (negative) value when $\omega t = \pi/2$ (Figure 2*b*).

In physical terms, model 1 and model 2 are equivalent because a positive perturbation in strength (model 1) is precisely equivalent to a negative perturbation in load (model 2). Mathematically, the two models are equivalent because in both cases the initiation time t_I is the smallest solution of the equation

$$x_0 + A \sin \omega t_I = m(t_I - t_T) \qquad (3)$$

For the remainder of this paper we shall derive results in which the origin of the time axis is chosen so that equation 3 is valid and the periodic part of the strength is increasing at $t = 0$. It is important to emphasise how this choice of the time origin might be made in practice for a given periodic process. In general, the periodic process (e.g. the ocean tide) is known as a function of time although it may not be known *a priori* whether it affects the 'load' $x_L(t)$ or the 'strength' $x_S(t)$. To choose an origin for the time axis which is consistent with equation 3 it is therefore necessary to make one of two assumptions: (1) the periodic process affects the strength $x_S(t)$, or (2) the periodic process affects the load $x_L(t)$. Since a positive perturbation in load is equivalent to a negative perturbation in strength the difference between assumptions (1) and (2) is simply translation in time by half a period π/ω. It follows that any predictions made about the distribution of initiation times under assumption (1) will differ from those made under assumption (2) by half a period.

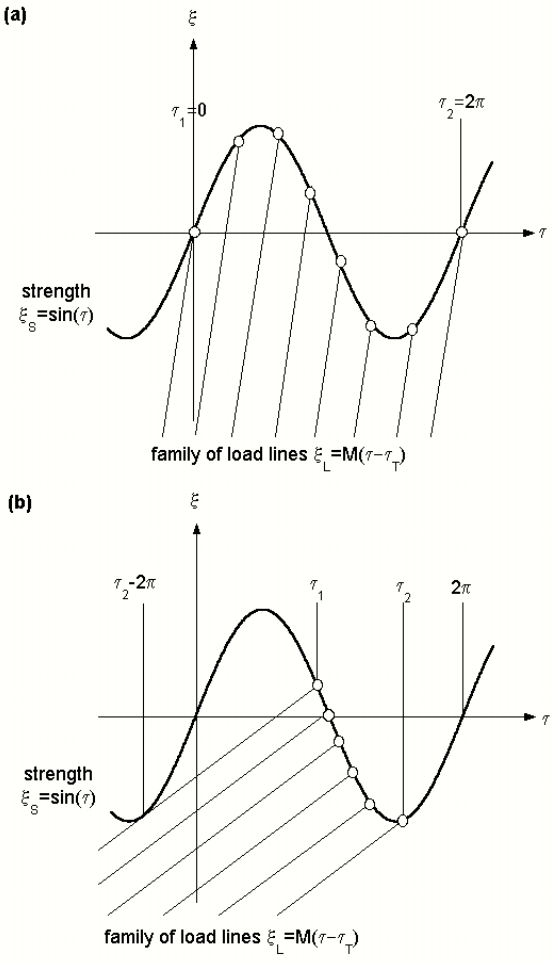

Figure 3. Sketches of the dimensionless model showing how the range of the initiation times depends on the dimensionless rate M. The load lines (for various values of the dimensionless time translation parameter τ_T) are shown as thin lines and the strength curve is shown as a thick line. Initiation events for each value of τ_T are indicated by open circles. (*a*) If $M \geq 1$ initiation events are possible at all dimensionless times in the range $[0, 2\pi]$; (*b*) If $M < 1$, initiation events are possible only at dimensionless times in the limited range $[\tau_1, \tau_2]$.

It is helpful to recast the model in dimensionless form by defining the dimensionless quantities

$$\xi = \frac{x - x_0}{A},\ \tau = \omega t,\ \tau_T = \omega\left(t_T + \frac{x_0}{m}\right) \tag{4}$$

and a 'dimensionless rate'

$$M = \frac{m}{A\omega} \tag{5}$$

The dimensionless rate M can be interpreted as the ratio of the rate of change of the linear process m to the maximum rate of change of the periodic process $A\omega$. It follows from equation 1 that the dimensionless governing equations are

$$\text{models 1 \& 2}: \begin{cases} \xi_L(\tau) &= M(\tau - \tau_T) \\ \xi_S(\tau) &= \sin\tau \end{cases} \tag{6}$$

and that the dimensionless initiation time $\tau_I = \omega t_I$ is the smallest solution of the equation:

$$\sin\tau_I = M\left(\tau_I - \tau_T\right) \tag{7}$$

In geometrical terms, an initiation event occurs when the linearly increasing dimensionless load $\xi_L(\tau)$ first exceeds the dimensionless strength $\xi_S(\tau)$ (Figure 3). The initiation time τ_I is therefore a function of the dimensionless rate M and the time translation parameter τ_T. It seems reasonable to assume that the physical processes controlling the periodic oscillations in strength and the linear increase in load are independent. It then follows that the problem is periodic in time and has translational symmetry along the time axis. We can therefore restrict attention to the dimensionless time interval $[0, 2\pi]$. It is then reasonable to assume that the time translation parameter τ_T is a random variable drawn from a uniform distribution on the interval $[0, 2\pi]$. Similarly, the dimensionless initiation time $\tau_I = \omega t_I \bmod 2\pi$, the dimensionless response time $\tau_R = \omega t_R \bmod 2\pi$ and the dimensionless failure time $\tau_F = \omega t_F \bmod 2\pi$ can all be viewed as radian angles in the range $[0, 2\pi]$. (We note, however, that it may sometimes be easier to express these radian angles in degrees so that they lie in the range $[0°, 360°]$). The statistical distributions of the dimensionless times τ_I, τ_R and τ_F will be investigated using the terminology of directional statistics [Mardia and Jupp, 2000].

Figure 3 shows that we expect two distinct regimes according to the size of the dimensionless rate M. If $M \geq 1$ (Figure 3*a*), the rate of increase of the load is sufficiently large that all initiation times in the range $[0, 2\pi]$ are possible. On the other hand, if $M < 1$ (Figure 3*b*) the rate of increase of the load is sufficiently small that certain initiation times become 'masked' by the curvature of the sine wave and initiation events are restricted to occur over a smaller interval.

3. The distribution of the initiation times

We show in detail in Appendix A how the model described above can be used to derive the probability density function (PDF) of the distribution of the initiation times as a function of the dimensionless rate M. We present a summary of these results here. Firstly, we define the constant τ_M by

$$\tau_M = \begin{cases} \cos^{-1}(M) & \text{if } M \leq 1 \\ 0 & \text{otherwise,} \end{cases} \tag{8}$$

It can then be shown (equations A13, A15 and A14) that the maximum initiation time τ_2 (in $[0, 2\pi]$) is

$$\tau_2 = 2\pi - \tau_M, \tag{9}$$

and that the minimum initiation time τ_1 is the solution (in $[0, 2\pi]$) of the equation

$$\sin\tau_1 - M\tau_1 = -\left(\sin\tau_M - M\tau_M\right). \tag{10}$$

The PDF of the dimensionless initiation times (on the interval $[0, 2\pi]$) is then:

$$f_I(\tau; M) = \begin{cases} \frac{1}{2\pi}\left(1 - \frac{\cos\tau}{M}\right) & \text{for } \tau_1 \leq \tau \leq \tau_2 \\ 0 & \text{otherwise.} \end{cases} \tag{11}$$

If the dimensionless rate is large ($M \geq 1$), then $\tau_1 = 0$, $\tau_2 = 2\pi$ and equation 11 reduces to the PDF of a distribution known in directional statistics as the 'cardioid distribution' [Mardia and Jupp (2000), Section 3.5.5; Jeffreys (1961), Section 5.94]. We therefore refer to the distribution in equation 11 as a 'pure cardioid distribution' if $M \geq 1$. On the other hand, we are not aware of any previous reference to a PDF of this form if $M < 1$. We therefore refer to the distribution as an 'extended cardioid distribution' if $M < 1$. The PDFs of pure and extended cardioid distributions are shown in Figure 4 for various values of the dimensionless rate M.

Figure 4*a* shows the minimum and maximum initiation times τ_1 and τ_2 as functions of the dimensionless rate M. If $M \geq 1$, all initiation times in the range $[0, 2\pi]$ are possible (Figure 3*a*). If $M < 1$, however, the initiation times are constrained to occur in a range of dimensionless times around $3\pi/2$ (Figure 3*b*).

Statistical distributions on the interval $[0, 2\pi]$ can be interpreted as distributions of vectors lying on the unit circle [Mardia and Jupp, 2000]. Consequently, the random variables τ_I, τ_R and τ_F which represent times in a periodic cycle can be interpreted as points on a 'clock face'. Given a sample of times drawn from such a distribution it is intuitively reasonable to characterise the sample by considering the magnitude and direction of the sum of the vectors corresponding to each of the observations in the sample. (We discuss this sample statistic further in the context of equation 32). The population equivalents of these sample statistics can be calculated by considering the 'first trigonometric moments' of the distribution:

$$C = \int_0^{2\pi} \cos(\theta) f(\theta) \mathrm{d}\theta, \quad S = \int_0^{2\pi} \sin(\theta) f(\theta) \mathrm{d}\theta \tag{12}$$

where $f(\theta)$ is the PDF of the distribution. The mean resultant length $\rho \in [0, 1]$ and mean direction $\mu \in [0, 2\pi]$ of the distribution are then defined by the complex equation:

$$\rho\exp(i\mu) = C + iS, \quad \text{where} \quad i = \sqrt{-1}. \tag{13}$$

The mean direction μ is a measure of the 'average direction' of a circular distribution. Figure 4*a* shows the mean direction μ_I of the distribution of the initiation times (equation 11) as a function of the dimensionless rate M.

The mean resultant length ρ is a measure of the non-uniformity of the distribution. For example, the circular uniform distribution $f(\theta) \equiv 1/2\pi$ (for which all directions

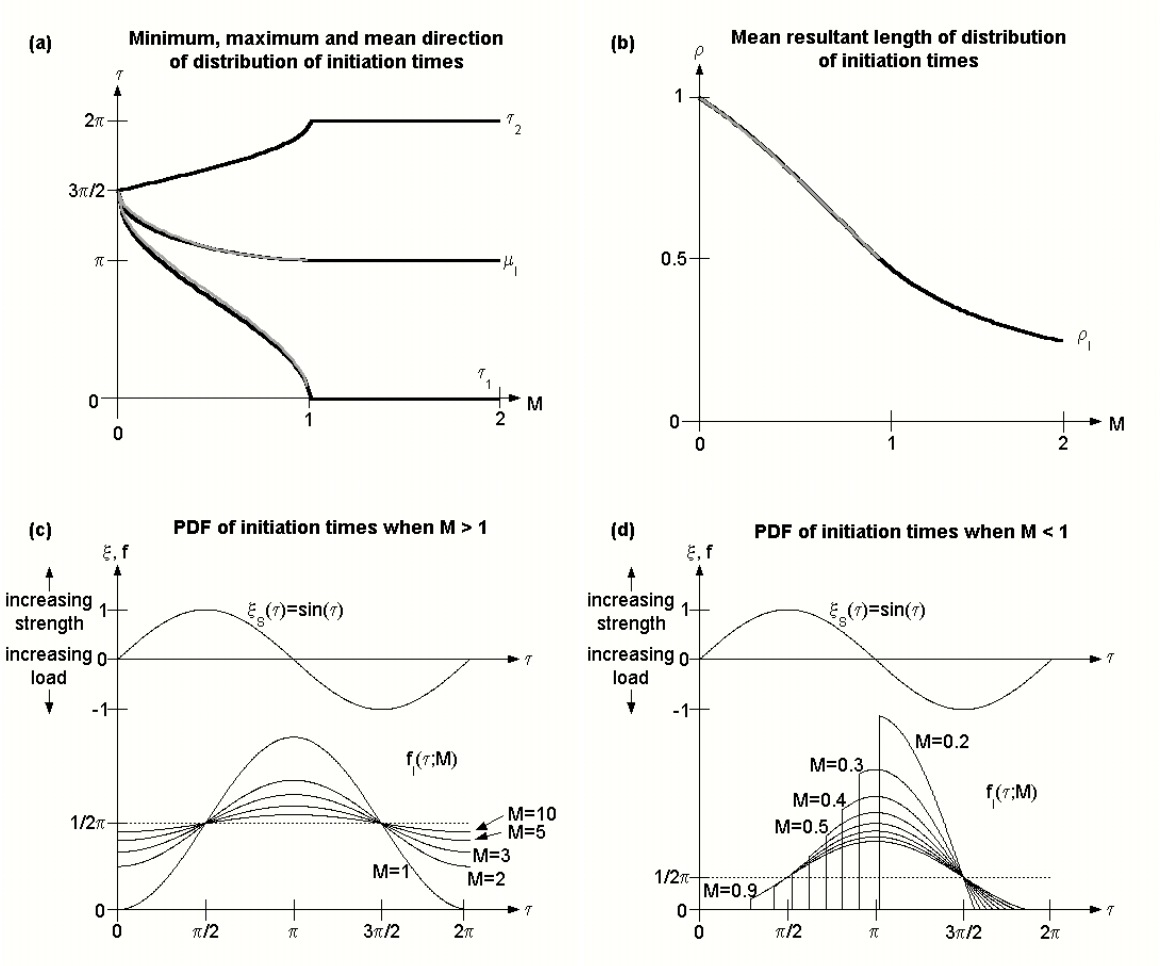

Figure 4. The properties of the PDF of the initiation times $f_I(\tau; M)$ as functions of the dimensionless rate M. (a) The minimum initiation time τ_1, the maximum initiation time τ_2 and the mean initiation time μ_I. Exact (analytical or numerical) results are shown in black. Where appropriate, the approximate functional forms of equation 15 are shown in grey; (b) The mean resultant length of the distribution of the initiation times ρ_I as a function of M. Exact solution in black, approximate solution of equation 15 in grey; (c) The PDF of the initiation times $f_I(\tau; M)$ for different values of M when $M \geq 1$. The periodic variations in load / strength are shown above for comparison ; (d) As part (c), but for $M < 1$.

are equally probable) has mean resultant length $\rho = 0$, while the pure cardioid distribution of equation 11 (if $M \geq 1$) has mean resultant length $1/2M$. Figure 4b shows the mean resultant length ρ_I of the distribution of the initiation times as a function of the dimensionless rate M. The mean resultant length ρ_I tends to zero as M tends to infinity. This corresponds to the limit in which the maximum rate $A\omega$ of the periodic process is negligibly small compared with the rate m of the linear process. Thus, for very large values of M the distribution of the initiation times is approximately uniform on $[0, 2\pi]$. On the other hand the mean resultant length ρ_I tends to unity as M tends to zero. This corresponds to the limit in which the maximum rate $A\omega$ of the periodic process is much larger than the rate m of the linear process. In this limit the periodic process has a very significant effect on the distribution of the initiation times, which becomes highly non-uniform.

Figures 4c,d show typical PDFs of the initiation times $f_I(\tau; M)$. The PDFs for various values of M are shown, along with graphs of the oscillations in the 'strength' fucntion for comparison. The uniform PDF $1/2\pi$ corresponding to the limit $M \to \infty$ is shown as a dotted line. Physically, this limit occurs when the periodic process has a negligible influence on the initiation time and all initiation times become equally probable. Figure 4c shows the PDFs if $M \geq 1$. In this case the PDF of the initiation times is a pure cardioid so it is sinusoidal in shape and symmetric in time about $\tau = \pi$. In general, therefore, initiation events are 'most probable' at dimensionless times $\tau \approx \pi$. This corresponds to the time in the periodic cycle when the oscillatory part of the strength is decreasing (model 1) or the oscillatory part of the load is increasing (model 2). On the other hand, initiation events are least probable at dimensionless times $\tau \approx 0$ (or, equivalently, $\tau \approx 2\pi$). This corresponds to periods when the oscillatory part of the strength is increasing (model 1) or the oscillatory part of the load is decreasing (model 2).

Equations 12 and 13 can be used to calculate the mean result length ρ_I and mean direction μ_I of the distribution of the initiation times (equation 11):

$$\left.\begin{array}{ll} \tau_1 = 0, & \tau_2 = 2\pi \\ \rho_I = \frac{1}{2M}, & \mu_I = \pi \end{array}\right\} \quad \text{if} \quad M \geq 1 \tag{14}$$

For example, if $M = 10$ then equation 11 shows that the distribution of the initiation times displays a 'fractional

non-uniformity' $1/M = 0.1$ while equation 14 shows that the mean resultant length is precisely half of this value: $\rho_I = 1/2M = 0.05$.

Figure 4*d* shows typical PDFs of the initiation times $f_I(\tau; M)$ if $M < 1$. Some initiation times are impossible (that is, they occur with probability zero) and the PDF is asymmetric in time. As $M \to 0$ the influence of the periodic process increases and the 'most probable' time for initiation events to occur moves from $\tau \approx \pi$ to $\tau \approx 3\pi/2$. In other words, as $M \to 0$ initiation events are restricted to occur within an ever-narrowing band of dimensionless times around $3\pi/2$. This represents the time in the periodic cycle when the oscillatory part of the strength takes its most negative value (model 1) or the oscillatory part of the load takes its most positive value (model 2).

When $M \geq 1$ the properties of the pure cardioid distribution listed in equation 14 can all be evaluated analytically. This is not the case when $M < 1$ and the initiation times are drawn from an extended cardioid distribution. The minimum initiation time τ_1 must be evaluated numerically from equation 10, and so the mean initiation time μ_I and the mean resultant length ρ_I also require numerical evaluation. Nonetheless it is possible to find functional forms which are an approximate fit to the numerically derived results. By using this method where necessary, we obtain the following mixture of analytical and approximate results for the extended cardioid distributions (when $M < 1$):

$$\left.\begin{aligned} \tau_1 &\approx \tfrac{3}{2}\cos^{-1}(2M-1) \\ \tau_2 &= 2\pi - \cos^{-1}(M) \\ \rho_I &\approx \sqrt{1-\tfrac{3M}{4}} \\ \mu_I &\approx \tfrac{\pi}{2}\left[3-\sqrt{M}+\tfrac{1}{2}M(M-1)\right] \end{aligned}\right\} \quad \text{if } M<1 \quad (15)$$

Figures 4*a,b* suggest that the errors introduced by using the approximate functional forms in equation 15 are small. Numerical calculations show that the approximations in equation 15 give errors of at most 0.04 for ρ_I and at most 0.122 radians (or 7°) for τ_1 and μ_I.

In summary, the distribution of the initiation times (Figure 4, equations 14,15) depends on the dimensionless rate M as follows. In the limit $M \to \infty$ the influence of the periodic process disappears and the initiation times become uniformly distributed on $[0, 2\pi]$. For finite values of M however, the initiation times are not uniformly distributed and have a mean direction μ_I in the range $[\pi, 3\pi/2]$. Initiation events are 'most probable' at a point between the time of decreasing strength $\tau = \pi$ and the time of minimum strength $\tau = 3\pi/2$. When $M \geq 1$ all initiation times are possible and the distribution of initiation times departs from uniformity by a factor $1/M$ (so that the mean resultant length is $\rho_I = 1/2M$)). The 'most probable' time for initiation events in this case is $\tau = \pi$. On the other hand, when $M < 1$ some initiation times are impossible and the distribution departs more significantly from uniformity. The range of possible initiation times becomes concentrated around $\tau = 3\pi/2$ as $M \to 0$.

Table 1 shows the rates $A\omega$ of several periodic processes of geophysical interest. We note in particular that the rate of loading by semi-diurnal ocean tides is several orders of magnitude greater than the rates due to other, longer period processes. Thus, if it is reasonable to assume that the same linear rate m is applicable on all timescales in Table 1, we should expect value of the dimensionless rate M to be several orders of magnitude smaller for semi-diurnal tidal loading than for the other processes. This would then imply that the non-uniformity (and hence mean resultant length ρ_I) in the initiation times should be significantly greater for tidal processes than for the longer period processes. At first sight, this may seem strange given that the evidence for non-uniformity is stronger at the annual timescale than it is at the tidal timescale. We propose that the resolution of this apparent paradox lies in the fact that it is 'failure events' rather than 'initiation events' which are observed and recorded. In particular, we shall show below that it is quite possible for the distribution of the initiation times to be highly non-uniform, but for the distribution of the failure events to be very close to uniform.

3.1. The distribution of the initiation times when M is drawn from a distribution

The distribution of the initiation times in equation 11 was derived under the assumption that the load function could be assumed to increase *linearly* on the timescale of the periodic process, so that the dimensionless rate M could be considered to be fixed. We now consider briefly the effect of relaxing this assumption. In a geophysical context, different values of M might occur at different locations (and at different times) because of variations in geological conditions or differences in the physical processes leading to an initiation event. We stress that we consider the value of M related to any particular initiation event to be deterministic, although it is almost certainly unknown. We are concerned with the statistics of a very large number of different initiation events (such as those corresponding to all recorded volcanic eruptions above a certain magnitude). It seems reasonable, therefore, to extend the results derived above by allowing the dimensionless rate M to be a random variable in the range $[0, \infty)$ drawn from some distribution with PDF $g(M)$. It then follows that the PDF of the initiation times should take the modified form

$$\hat{f}_I(\tau) = \int_0^\infty g(M) f_I(\tau; M) \mathrm{d}M \quad (16)$$

where the PDF $f_I(\tau; M)$ is given by equation 11. In general terms, the integral in equation 16 shows that $\hat{f}_I(\tau)$ is a 'weighted average' of individual PDFs $f_I(\tau; M)$. Thus, if we had some reason to suppose that the dimensionless rate M were 'usually' greater than unity, we might expect the PDF $\hat{f}_I(\tau)$ to be dominated to the contribution of the pure cardioid PDFs in figure 4*c*, and so $\hat{f}_I(\tau)$ would itself be approximately a pure cardioid. On the other hand, if M were less than unity 'sufficiently often', we might expect the extended cardioid PDFs of figure 4*d* to have a significant effect on the integral and for the PDF $\hat{f}_I(\tau)$ to be noticeably asymmetric.

To illustrate this principle we consider one special case which yields a simple result. If the distribution of rates $g(M)$ happens to be of such a form that dimensionless rates less than unity never occur (i.e. $g(M) = 0$ for all $M < 1$), then equation 16 reduces to the simpler form

$$\hat{f}_I(\tau) = \frac{1}{2\pi}\left[1 - \left[\int_1^\infty \frac{g(M)}{M}\mathrm{d}M\right]\cos\tau\right] \quad (17)$$

In this case the PDF $\hat{f}_I(\tau)$ is simply a pure cardioid distribution of the form given in equation 11 except that the

parameter M^{-1} in equation 11 has simply been replaced by its mean value $E[M^{-1}]$.

Unfortunately, it is not clear what form the PDF of the rates $g(M)$ is likely to take in any particular geophysical application of this theory. Nonetheless, the use of equation 16 can be illustrated with a specific example which is at least physically plausible. We suppose for simplicity that there exists some minimum rate M_0. In physical terms, we imagine that the existence of some 'long period' physical process ensures that the linear rate of increase m cannot drop below a level corresponding to this limiting process. We then suppose for illustrative purposes that M is drawn from a Pareto distribution with shape parameter $\alpha > 0$, so that the PDF of the rates is

$$g(M) = \alpha M_0^{\alpha} \frac{1}{M^{1+\alpha}}, \; M \in [M_0, \infty) \tag{18}$$

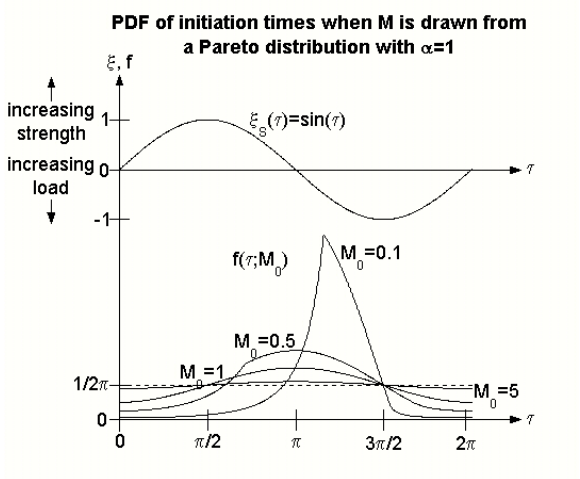

Figure 5. The PDF of the initiation times $\hat{f}_I(\tau)$ when M is drawn from a Pareto distribution (equation 18) with shape parameter $\alpha = 1$. PDFs are shown for various values of the minimum rate M_0. Periodic variations in strength are shown above for comparison.

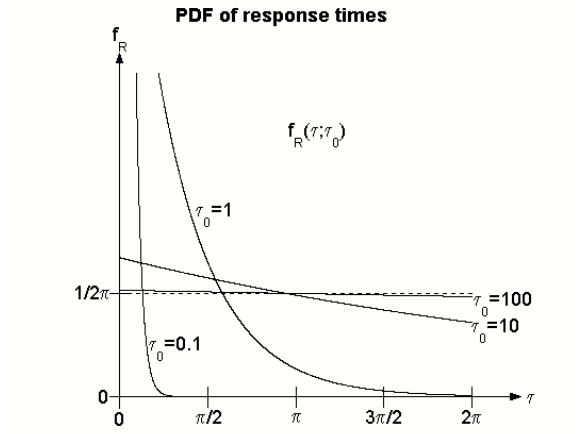

Figure 6. The PDF of the distribution of the dimensionless response times $f_R(\tau;\tau_0)$ if the response times are drawn from the wrapped exponential distribution of equation 22.

By way of heuristic physical justification for this functional form, we note solely that the Pareto family of distributions has density functions which are 'negative powers' of the random variable. Such power-law distributions occur frequently in physics when processes are distributed over a wide range of scales.

If $M_0 \leq 1$, it is possible for the dimensionless rate M to take values less than unity and the integral in equation 16 must be evaluated numerically. If $M_0 \geq 1$, however, we can use equation 17 to get the simple expression

$$\hat{f}_I(\tau) = \frac{1}{2\pi}\left[1 - \left(\frac{\alpha}{1+\alpha}\right)\frac{1}{M_0}\cos\tau\right] \quad \text{if} \quad M_0 \geq 1 \tag{19}$$

In other words, if the minimum rate M_0 is greater than unity, the PDF $\hat{f}_I$ is a weighted average of pure cardioid PDFs and is itself a pure cardioid. Conversely, if it is possible for M to take values less than unity, the PDF $\hat{f}_I$ loses its symmetry and becomes 'peaked' near $\tau = 3\pi/2$. Some examples of PDFs $\hat{f}_I(\tau)$ derived in this way are shown in Figure 5*b* in the case $\alpha = 1$ (so that $g(M) \sim 1/M^2$). PDFs $\hat{f}_I(\tau)$ are shown for various values of the minimum rate parameter M_0.

In summary, it is possible to treat the dimensionless rate M as a random variable with PDF $g(M)$ in which case the distribution of the initiation times has a PDF of the form given in equation 16. We suggest, however, that unless the distribution $g(M)$ is known there is little to be gained by doing so. For example, if M is a random variable drawn from a Pareto distribution with minimum rate $M_0 \geq 1$ and shape parameter α, then the resulting distribution of the initiation times $f_I(\tau; M)$ is indistinguishable from that which arises when the parameter M is assigned the constant value $\alpha/M_0(1+\alpha)$.

For this reason, we shall assume for the remainder of this paper that the dimensionless rate M is fixed.

4. The distribution of the response times

In the previous section we discussed the statistical distribution of the (dimensionless) initiation times $f_I(\tau; M)$. We now consider the distribution of the (dimensional) response time t_R, which is the length of time which elapses between an initiation event and a failure event (Figures 1,2). We treat the response time as a random variable in the range $[0, \infty)$ drawn from a statistical distribution with PDF $\tilde{f}_R(t)$. Of course, the precise form of this distribution depends on the physics of the failure process, which may be unknown. Nonetheless it is possible to illustrate the general principles of this approach by assuming a particular functional form for the distribution of the response times. Specifically, we suppose for simplicity that the response times are drawn from an exponential distribution with mean response time t_0. The exponential distribution is arguably the simplest of all distributions representing a failure process since it has a constant hazard function (i.e. the probability of failure in a small time interval $[t, t+dt]$, given that no failure has occurred before time t, is dt/t_0 [Kalbfleisch and Prentice, 1980]). Assuming then that the response times are drawn from an exponential distribution it follows that the PDF of the (dimensional) response times is

$$\tilde{f}_R(t; t_0) = \frac{1}{t_0}\exp\left(\frac{-t}{t_0}\right) \tag{20}$$

It is helpful to nondimensionalise the response time t_R and the mean response time t_0 using the angular frequency of

the periodic process ω:

$$\tau_R = \omega t_R, \quad \tau_0 = \omega t_0 \tag{21}$$

As in previous sections, we can consider the dimensionless response time τ_R to lie within the restricted range $[0, 2\pi]$ provided that we replace the exponential distribution of equation 20 with an appropriately wrapped circular distribution [Mardia and Jupp, 2000]. It can then be shown that the distribution of the dimensionless response times τ_R (on the interval $[0, 2\pi]$) is given by the wrapped exponential distribution [Jammalamadaka and Kozubowski, 2001]:

$$f_R(\tau; \tau_0) = \frac{\exp\left(\frac{-\tau}{\tau_0}\right)}{\tau_0\left(1 - \exp\left(\frac{-2\pi}{\tau_0}\right)\right)} \tag{22}$$

Graphs of this wrapped exponential PDF are shown for several values of the dimensionless mean response time τ_0 in figure 6. It can be shown that the mean resultant length ρ_R and mean direction μ_R of this wrapped exponential distribution are given [Jammalamadaka and Kozubowski, 2001] by:

$$\rho_R = \frac{1}{\sqrt{1+\tau_0^2}}, \quad \mu_R = \tan^{-1}\tau_0 \tag{23}$$

In summary, if the response time is assumed to be drawn from a wrapped exponential distribution then its distribution depends on a single parameter: the dimensionless mean response time τ_0. If $\tau_0 \approx 0$ the response time is negligibly short compared to the period of the periodic process and we should expect the dimensionless failure time τ_F to be approximately equal to the dimensionless initiation time τ_I. In this case the distribution of the failure times will be controlled by (and approximately equal to) the distribution of the initiation times. On the other hand, for larger values of the dimensionless mean response time τ_0 we expect the response time to have a significant effect and for the distribution of the failure times to differ from the distribution of the initiation times. In particular, in the limit $\tau_0 \to \infty$ the distribution of the response times approaches the uniform circular distribution. In this case we should expect the distribution of the failure times to be approximately uniform also, even if the distribution of the initiation times is highly non-uniform.

5. The distribution of the failure times

The dimensionless failure time τ_F is by definition the sum of the dimensionless initiation time τ_I and the dimensionless response time τ_R (considered mod 2π). Since all three of these quantities are regarded as random variables on the interval $[0, 2\pi]$, it follows [Mardia and Jupp, 2000] that the PDF of the failure time is given by the convolution:

$$\begin{aligned} f_F(\tau; M, \tau_0) &= \int_0^{\tau} f_I(s; M) f_R(\tau - s; \tau_0) ds \\ &+ \int_{\tau}^{2\pi} f_I(s; M) f_R(2\pi + \tau - s; \tau_0) ds \end{aligned} \tag{24}$$

Equations 11 and 22 can therefore be combined using equation 24 to give the PDF of the distribution of the failure times:

$$f_F(\tau; M, \tau_0) = \begin{cases} A\exp\left(\frac{-\tau}{\tau_0}\right) & \tau \in [0, \tau_1) \\ h(\tau) + B\exp\left(-\frac{\tau}{\tau_0}\right) & \tau \in [\tau_1, \tau_2] \\ A\exp\left(\frac{2\pi - \tau}{\tau_0}\right) & \tau \in (\tau_2, 2\pi] \end{cases} \tag{25}$$

where the function $h(\tau)$ takes the form of a 'pure cardioid' PDF:

$$h(\tau) = \frac{1}{2\pi}\left[1 - \frac{\cos\left(\tau - \tan^{-1}\tau_0\right)}{M\sqrt{1+\tau_0^2}}\right] \tag{26}$$

and where the constants A and B are defined by:

$$\begin{aligned} A &= \frac{h(\tau_2)\exp\left(\frac{\tau_2 - 2\pi}{\tau_0}\right) - h(\tau_1)\exp\left(\frac{\tau_1 - 2\pi}{\tau_0}\right)}{1 - \exp\left(\frac{-2\pi}{\tau_0}\right)} \\ B &= \frac{h(\tau_2)\exp\left(\frac{\tau_2 - 2\pi}{\tau_0}\right) - h(\tau_1)\exp\left(\frac{\tau_1}{\tau_0}\right)}{1 - \exp\left(\frac{-2\pi}{\tau_0}\right)} \end{aligned} \tag{27}$$

Equation 25 shows that the PDF of the distribution of the failure times takes different forms inside and outside the interval $[\tau_1, \tau_2]$. Outside this interval, the PDF $f_F(\tau; M, \tau_0)$ has the form of a wrapped exponential distribution. Within the interval $[\tau_1, \tau_2]$, however, the PDF $f_F(\tau; M, \tau_0)$ is the sum of a 'pure cardioid' component $h(\tau)$ and a wrapped exponential component.

The theory of circular distributions [Mardia and Jupp, 2000] shows that the mean resultant length ρ_F and mean direction μ_F of the distribution of the failure time are given by:

$$\rho_F = \rho_I \rho_R, \quad \mu_F = \mu_I + \mu_R \tag{28}$$

The mean resultant length ρ_F and mean direction μ_F of the distribution of the failure times are shown as functions of the parameters M and τ_0 in Figure 7*a,b*. Equation 28 reveals how the distribution of the response times (equation 22) modifies the distribution of the initiation times (equation 11) to give the distribution of the failure times 25. The fact that $\mu_R = \tan^{-1}\tau_0$ implies that the mean failure time lags the mean initiation time by a radian angle $\tan^{-1}\tau_0$. Similarly, the effect of the mean resultant length ρ_R of the response time is make the mean resultant length of the failure times ρ_F less than the mean resultant length ρ_I of the initiation times by a factor $\sqrt{1+\tau_0^2}$. Thus, the non-uniformity of the failure times is always less than the non-uniformity of the initiation times.

If $M \geq 1$, then $\tau_1 = 0$, $\tau_2 = 2\pi$, $A = h(0)$ and $B = 0$. The PDF of the failure times (equation 25) then simplifies to:

$$f_F(\tau; M, \tau_0) = \frac{1}{2\pi}\left[1 - \frac{\cos\left(\tau - \tan^{-1}\tau_0\right)}{M\sqrt{1+\tau_0^2}}\right], \tag{29}$$

the mean resultant length and mean direction are:

$$\left.\begin{aligned} \rho_F &= \frac{1}{2M\sqrt{1+\tau_0^2}} \\ \mu_F &= \pi + \tan^{-1}\tau_0 \end{aligned}\right\} \text{ if } M \geq 1 \tag{30}$$

and it follows that the distribution of the failure times is a pure cardioid distribution (Figure 7*d*). If the mean response time is much less than the period of the periodic

process ($\tau_0 \ll 1$) then the response time of the system is negligible and the PDF of the failure times approaches the PDF of the initiation times. Thus, when $M \geq 1$ and $\tau_0 \ll 1$ the most probable failure time occurs when the strength is decreasing (Figures 7*b,d*). On the other hand, if the mean response time is much greater than the period ($\tau_0 \gg 1$) then the distribution of the failure times becomes more uniform than the distribution of the initiation times. In this case the most probable failure time moves towards the time of minimum strength / maximum load.

If $M < 1$ the PDF of the inititiation times is an extended cardioid and the PDF of the failure times takes the more complicated form shown in Figure 7*c*. Nonetheless, the same qualitative results hold as in the case when $M \geq 1$. When $\tau_0 \ll 1$ the response time is negligible and the distribution of the failure times is similar to the distribution of the initiation times. On the other hand, when $\tau_0 \gg 1$ the effect of the long response time is to smooth any non-uniformity in the initiation time and make the distribution of the failure times approach uniformity. It can be shown that

$$\left.\begin{aligned} \rho_F &\approx \frac{1}{2}\sqrt{\frac{4-3M}{1+\tau_0^2}} \\ \mu_F &\approx \frac{\pi}{2}\left[3-\sqrt{M}+\frac{1}{2}M(M-1)\right] \\ &+ \tan^{-1}\tau_0 \end{aligned}\right\} \text{ if } M < 1 \quad (31)$$

In summary, the properties of the distribution of the failure times are controlled by the dimensionless rate M (which controls the initiation time) and the dimensionless mean response time τ_0 (which controls the response time). When $M < 1$ the distribution of the initiation times is significantly non-uniform but the distribution of the failure times can nonetheless be close to uniform if τ_0 is sufficiently large.

6. Use of the model to estimate parameter values

In the previous sections we derived a complete statistical description of the distributions of the initiation, response and failure times under a number of simplifying assumptions (equations 11, 22, 25). We now present two examples of how this model can be used to estimate parameter values from geophysical data, if the magnitude A and angular frequency ω of the periodic process under consideration are known. We emphasise that a fitting procedure of this sort can never *prove* that a statistical model is a good representation of physical reality. Nonetheless, it is of interest to see what values of the controlling parameters M and τ_0 are consistent with a given set of observations under the *assumption* that the model is valid.

In general, the data in an investigation of periodic behaviour consist of a set $\{t_{F,1}, \ldots, t_{F,n}\}$ of 'failure times' such as the times at which earthquakes have occurred or volcanoes have erupted. In order to apply the model developed here we assume that any non-uniformity at angular frequency ω is caused by a known periodic process (such as changes sea level or barometric pressure) of amplitude A which might plausibly affect a 'load function' or a 'strength function'. We can then nondimensionalise the data by defining the set of dimensionless failure times $\{\tau_{F,i} = \omega(t_{F,i} - t_p) \pmod{2\pi}\}$. The phase parameter t_p is chosen so that a dimensionless failure time $\tau_F = 0$ corresponds to the time in the periodic cycle at which the periodic process is increasing (if positive values correspond to increased 'load') or decreasing (if positive values correspond to increased 'strength'). We stress again that the results differ by a phase angle π (or 180°) according to whether the periodic process is assumed to affect the load or the strength. Once the failure times have been nondimensionalised, the (sample) first trigonometric moments can be calculated:

$$\bar{C} = \frac{1}{n}\sum_{j=1}^{n}\cos\tau_{F,j}, \qquad \bar{S} = \frac{1}{n}\sum_{j=1}^{n}\sin\tau_{F,j}. \quad (32)$$

These are the sample equivalents of the population moments given in equation 12. The (sample) mean resultant length $\bar{R}$ and the (sample) mean direction $\bar{\theta}$ are then given by

$$\bar{R}\exp(i\bar{\theta}) = \bar{C} + i\bar{S} \quad (33)$$

which is the sample equivalent of equation 13. The aim now is to use the data to produce estimates $\hat{M}$ and $\hat{\tau}_0$ of the two dimensionless parameters M and τ_0 in the model for the failure times. A reasonable strategy is to demand that the model have the same first trigonometric moments as the data. Accordingly, we define $\hat{M}$ and $\hat{\tau}_0$ to be the values of M and τ_0 for which $\mu_F = \bar{\theta}$ and $\rho_F = \bar{R}$. The principle of this inversion is illustrated by the plots in Figure 7*a,b*. Observed values of the mean resultant length $\bar{R}$ and mean direction $\bar{\theta}$ constrain the model parameters M and τ_0 so that ρ_F and μ_F lie on the contours corresponding to $\bar{R}$ and $\bar{\theta}$ in Figures 7*a,b*. In theory, therefore, measured values of $\bar{R}$ and $\bar{\theta}$ could be used to infer values of $\hat{M}$ and $\hat{\tau}_0$. In practice, of course, measured values of $\bar{R}$ and $\bar{\theta}$ have associated error bars and so it will only be possible to specify a range of values of $\hat{M}$ and $\hat{\tau}_0$ which are consistent with the data. In the following sections we illustrate this principle with two specific examples.

6.1. Annual periodicity in volcanic eruptions

We now present an interpretation of some data for the frequency of volcanic eruptions. We consider periodic processes on two timescales: an annual period of 365 days (denoted by the subscript 'a') and a tidal period of 12 hours (denoted by the subscript 't'). Mason *et al.* (2002) suggest that the monthly rate of volcanic eruptions varies by about ±10% over the course of a year and so the sample mean resultant length (at the annual timescale) is $\bar{R}_a = 0.05$. Their data also suggest that if annual changes in sea level are assumed to be the periodic process causing this non-uniformity, then $\bar{\theta}_a = 210° \pm 30°$. On the other hand, no strong evidence of non-uniformity on the (daily) tidal timescale has been found [Mason *et al.*, 2002] and so we expect that the sample mean resultant length on the tidal timescale should be much smaller: $\bar{R}_t \ll 0.05$.

We now assume that the dominant periodic processes on these timescales are annual variations in barometric pressure and tidal variations in sea level. From Table 1 we deduce that reasonable parameter values are:

$$\begin{aligned} A_a &= 1000 \text{ Pa}, \quad \omega_a = 2\cdot 10^{-7} \text{ rad.s}^{-1} \\ A_t &= 10,000 \text{ Pa}, \quad \omega_t = 1.45\cdot 10^{-4} \text{ rad.s}^{-1} \end{aligned} \quad (34)$$

We can now use the theory developed in the previous sections to estimate a typical linear rate of stress increase at volcanoes m and a typical mean response time t_0 of volcanoes to an initiation event. Our constraints are $\rho_{F,a} = 0.05$,

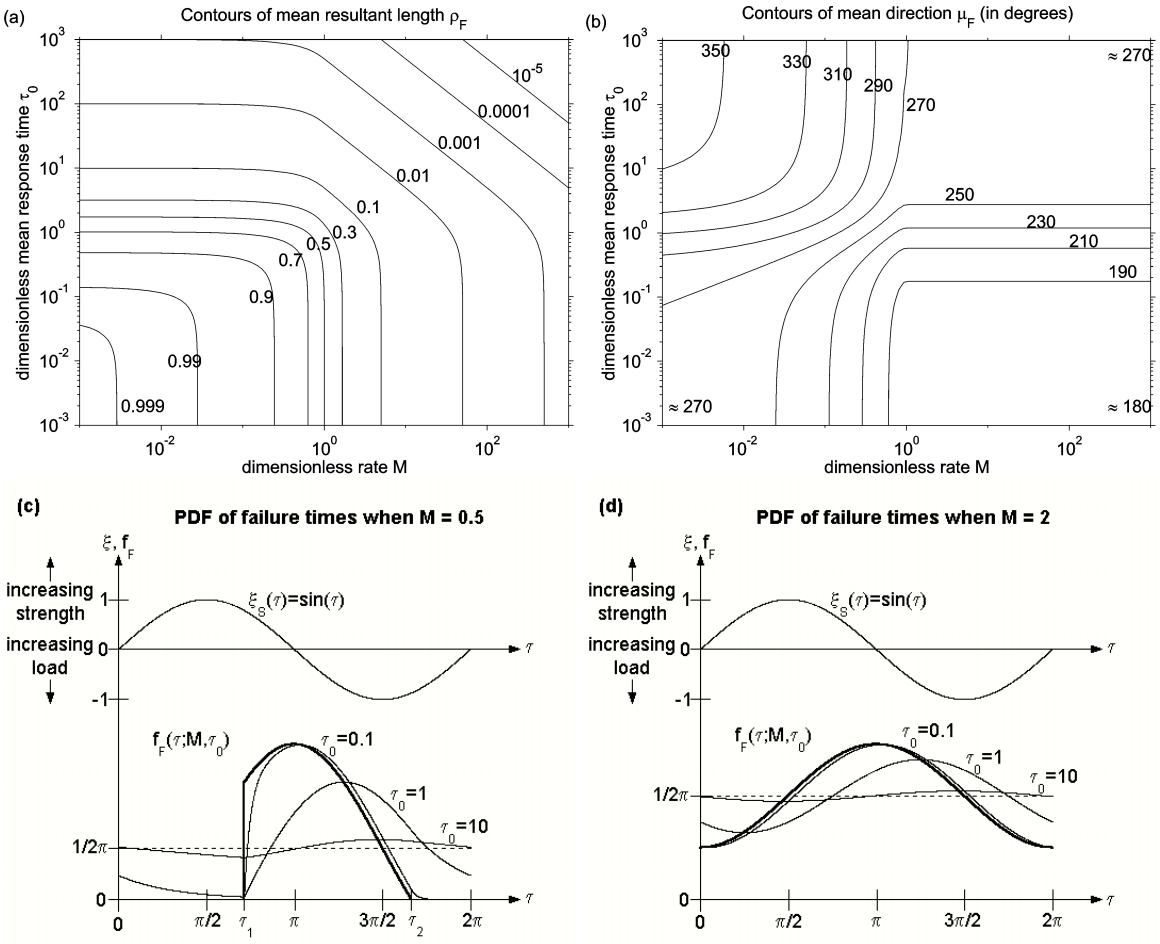

Figure 7. Properties of the distribution of failure times $f_F(\tau; M, \tau_0)$ as functions of the dimensionless rate M and the dimensionless mean response time τ_0. (a) Contours of the mean resultant length ρ_F; (b) Contours of the mean direction μ_F measured relative to the dimensionless time $\tau = 0$ at which the periodic part of the strength is increasing. Note that these contours are labelled in degrees rather than radians for ease of interpretation; (c) Examples of the PDF $f_F(\tau; M, \tau_0)$ in a case where $M < 1$ (thin lines). For comparison, the distribution of the initiation times $f_I(\tau; M)$ is shown as a thick line, and the uniform distribution is shown as a dotted line; (d) As for (c) but in a case where $M \geq 1$;.

$\mu_a = 210^\circ \pm 30^\circ$ and $\rho_{F,t} \ll 0.05$. The dimensionless rate and dimensionless mean response time are given at the two timescales by:

$$\begin{aligned} M_a &= \frac{m}{A_a \omega_a}, \quad \tau_{0,a} = \omega_a t_0 \\ M_t &= \frac{m}{A_t \omega_t}, \quad \tau_{0,t} = \omega_t t_0 \end{aligned} \tag{35}$$

and so equations 28 and 31 imply that

$$\begin{aligned} \tau_{0,a} &\approx \sqrt{\frac{4 - 3M_a}{4R_a^2} - 1} \quad \text{if} \quad M_a < 1 \\ \tau_{0,a} &= \sqrt{\frac{1}{4M_a^2 \bar{R}_a^2} - 1} \quad \text{if} \quad M_a \geq 1 \end{aligned} \tag{36}$$

For each possible value of m the mean failure times on both timescales can be calculated (Figure 8a) under the constraint $\rho_{F,a} = \bar{R}_a = 0.05$. Since $\mu_{F,a}$ is constrained by the observation $\bar{\theta}_a = 210^\circ \pm 30^\circ$ we deduce that the model is consistent with the observations for values of the dimensional rate m between $2 \cdot 10^{-3}$ Pa.s^{-1} and $4 \cdot 10^{-3}$ Pa.s^{-1}. We note that this range includes the 'typical rate of increase of tectonic stress' $m \sim 2.8 \cdot 10^{-3}$ Pa.s^{-1}) quoted by Vidale *et al.* (1998). Equations 35 and 36 can also be used to calculate the mean response time t_0 and the mean resultant length on the tidal timescale $\rho_{F,t}$ as a function of the rate m (Figure 8b). We note that the mean resultant length on the tidal timescale $\rho_{F,t}$ is less than 0.01 for all consistent values of the rate m, and that the mean response time t_0 is constrained to be less than about 100 days.

We have shown that the model developed above is consistent with observations of periodicity in volcanic activity provided that (1) the mean response time t_0 is less than about 100 days, and (2) the linear rate m lies between $2 \cdot 10^{-3}$ Pa.s^{-1} and $4 \cdot 10^{-3}$ Pa.s^{-1}. In order to give the observed mean resultant length $\bar{R}_a = 0.05$ the values of m and t_0 are constrained to lie on the line shown in Figure 8b. If m is at the lower end of the permissible range, then the distribution of the initiation times is relatively non-uniform and so the mean response t_0 must be relatively large in order to smooth out this non-uniformity to give the observed non-uniformity in the failure times. On the other hand, if m is at the upper end of the permissible range then mean response time t_0 must be so small that the influence of the response time is negligible. In this limit the non-uniformity in the

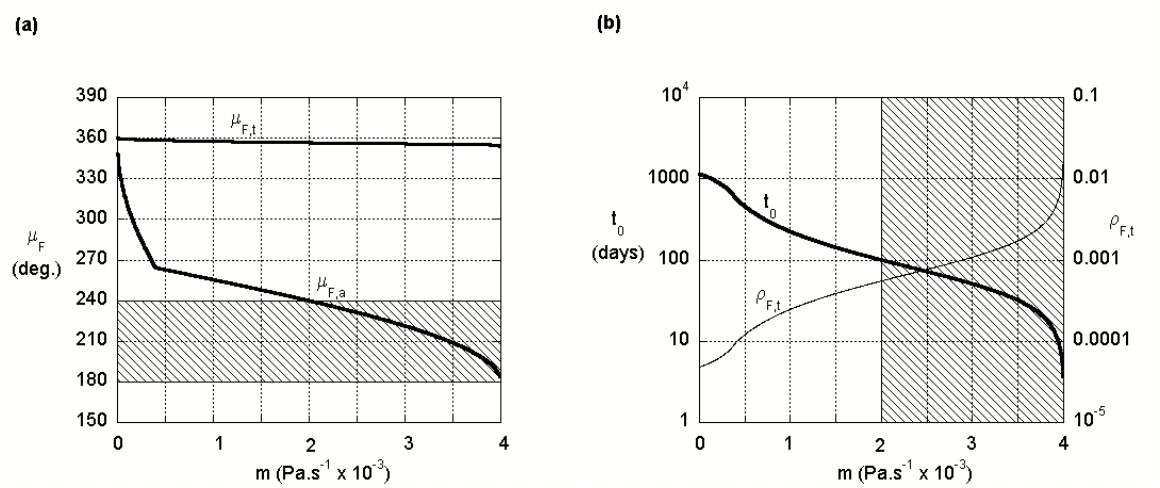

Figure 8. Figures illustrating the range of parameter values consistent with observations of periodicity in the rate of volcanic eruptions. Mason *et al.* (2002) consider mean sea level as the periodic process and find that the sample mean resultant length on an annual timescale is $\bar{R}_a = 0.05$ and the sample mean direction is $\bar{\theta}_a = 210^\circ \pm 30^\circ$. (*a*) The mean failure time on the annual timescale $\mu_{F,a}$ and the mean failure time on the tidal timescale $\mu_{F,t}$ as functions of the linear rate of stress accumulation m. It is assumed that positive crustal loads lead to positive perturbations in the load function $x_L(t)$. The range of the sample mean direction (shaded) suggests that m lies between $2 \cdot 10^{-3}$ Pa.s^{-1} and $4 \cdot 10^{-3}$ Pa.s^{-1}; (*b*) The (dimensional) mean response time t_0 and mean resultant length on the tidal timescale $\rho_{F,t}$ as functions of the linear rate m. The range of m deduced in (*a*) is shaded.

failure times is controlled entirely by the non-uniformity in the initiation times.

6.2. Seismicity following the Landers earthquake

We now discuss briefly a second example of some data to which our theory can be applied, this time in the context of seismic activity. Gao *et al.* (2000) report the number of seismic events per day in the Western USA following the Landers earthquake in 1992. They note a periodicity on an annual timescale in which the number of events per day varies annually by $\pm 30\%$ compared with the mean number of events per day. This corresponds to a sample mean resultant length $\bar{R}_a \approx 0.15$. Gao *et al.* (2000) correlate this non-uniformity with annual variations in local barometric pressure, noting that annual barometric pressure lows precede annual seismic highs by about 90 days (or $\approx 90^\circ$). This corresponds an observed mean failure time $\bar{\theta}_a = 180^\circ$ if it is assumed that barometric highs correspond to maxima in a 'load function' $x_L(t)$. Gao *et al.* (2000) suggest that this phase lag between barometric highs and peak seismicity is due to hydrological diffusion. We suggest an alternative explanation for this phase lag in terms of our model. We use the contour plots in figure 7 and equations 28, 31 to interpret their data. The observations $\bar{R}_a \approx 0.15$ and $\bar{\theta}_a = 180^\circ$ are consistent with a model of this form with $\tau_0 <\approx 1$ and $M \approx 3$. In dimensional terms, the constraint $\tau_0 <\approx 1$ means that the mean response time t_0 is less than about 58 days. The changes in barometric pressure have magnitude $A = 1$ kPa and angular frequency $\omega = 2 \cdot 10^{-7}$ rad.s^{-1}, and so the constraint $M \approx 3$ suggests a linear tectonic stress rate of $m \approx 6 \cdot 10^{-4}$ Pa.s^{-1}.

7. Conclusions

We have derived exact mathematical results from a simple model describing the influence of an external periodic process on the times at which generic 'failure events' (such as earthquakes and volcanic eruptions) occur.

In our model, an initiation event at the initiation time t_I occurs when a 'load' function exceeds a 'strength' function. Following the initiation event the system fails after a response time t_R so that the observed failure time is $t_F = t_I + t_R$. In the absence of any periodic process we assume for simplicity that the load and the strength approach each other linearly at rate m. The presence of the external periodic process imposes sinusoidal oscillations of the form $A \sin \omega t$ on either the load or the strength. The distribution of the initiation times is then given by equation 11 and is governed by the dimensionless rate $M = m/A\omega$. This parameter is the ratio of the rate of change of the linear process to the maximum rate of change of the periodic process. The distribution of the failure times then depends on the distribution of the response times. For simplicity, we consider the particular case where the response times are exponential distributed with mean response time t_0 (equation 22). In this case the distribution of the failure times (equation 25) is governed by two dimensionless parameters: the dimensionless mean response time $\tau_0 = \omega t_0$ and the dimensionless rate M.

Our model is deliberately simplistic, but we suggest that it provides a useful framework for interpreting evidence of periodicity in earthquakes and volcanic eruptions on a wide range of timescales.

Appendix A: Derivation of the PDF of the initiation times

If the dimensionless initiation time τ lies in a region where $\mathrm{d}\xi_S/\mathrm{d}\tau \geq 0$ then Figure 9*a* applies. We consider an infinitesimally small section of the load function $\xi_S(\tau)$ of length $\mathrm{d}s$. It follows from triangle KJL that

$$\tan \psi = \frac{\mathrm{d}\xi_S}{\mathrm{d}\tau} = \cos \tau \qquad \text{(A1)}$$

We now consider two load lines of rate M which correspond to initiation times τ and $\tau + \mathrm{d}\tau$. Both of these load lines lie at an angle θ to the τ-axis. It follows from triangle JNP that

$$\tan\theta = M \tag{A2}$$

Since we have assumed that τ_T is uniformly distributed on the interval $[0, 2\pi]$ it follows that the probability of a load line lying between lines 1 and 2 is $\mathrm{d}\tau_T/2\pi$. This is equal to the probability $f_I(\tau; M)\mathrm{d}\tau$ of an initiation event occurring in the interval $[\tau, \tau + \mathrm{d}\tau]$. We therefore deduce the general relationship

$$f_I(\tau; M) = \frac{1}{2\pi}\frac{\mathrm{d}\tau_T}{\mathrm{d}\tau} \tag{A3}$$

Consideration of triangles KJL and QLN shows that

$$\frac{\mathrm{d}\tau}{\mathrm{d}s} = \cos\psi, \quad \frac{\mathrm{d}\sigma}{\mathrm{d}\tau_T} = \sin\theta \tag{A4}$$

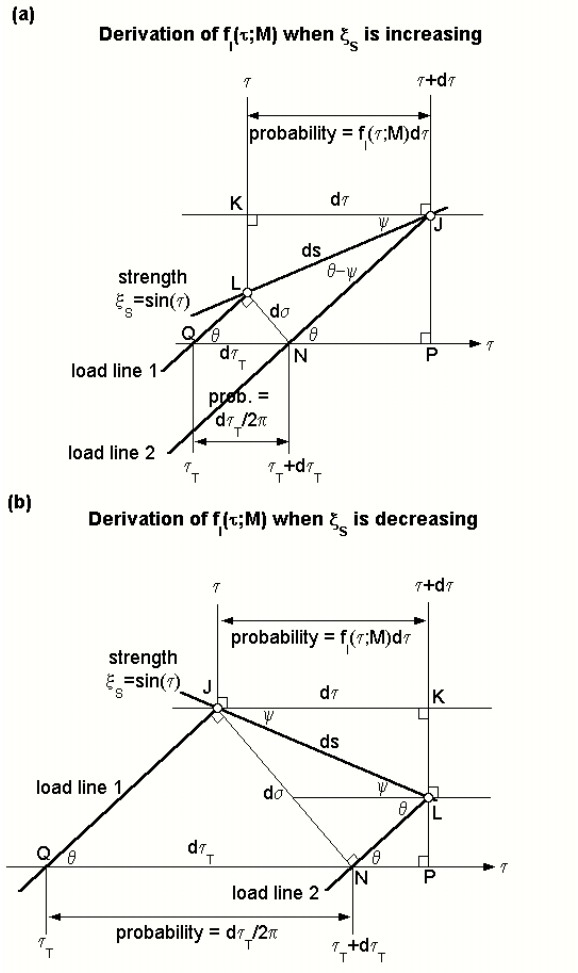

Figure 9. Sketch of the geometrical relations used in the derivation of the PDF of the initiation times $f_I(\tau; M)$. In both panels the strength curve is shown in bold running between J and L. Two load lines (corresponding to different values of the time translation parameter τ_T) are shown in bold and intersect the strength curve at J and L. The corresponding initiation events occur at times τ and $\tau + \mathrm{d}\tau$. (a) Sketch for the case $\mathrm{d}\xi_S/\mathrm{d}\tau \geq 0$; ($b$) Sketch for the case $\mathrm{d}\xi_S/\mathrm{d}\tau \leq 0$.

while triangle NJL implies that

$$\frac{\mathrm{d}\sigma}{\mathrm{d}s} = \sin(\theta - \psi) \tag{A5}$$

Using the identity $\sin(\theta - \psi) = \sin\theta\cos\psi - \cos\theta\sin\psi$, it follows from equations A2, A3, A4 and A5 that

$$f_I(\tau; M) = \frac{1}{2\pi}\left[1 - \frac{\tan\psi}{M}\right], \quad \text{if} \quad \frac{\mathrm{d}\xi_S}{\mathrm{d}\tau} \geq 0 \tag{A6}$$

If $\mathrm{d}\xi_S/\mathrm{d}\tau \leq 0$, a result analogous to equation A6 can be derived (Figure 9b). It is easily shown that equations A2, A3 and A4 apply as before but equation A1 must now be replaced by

$$\tan\psi = -\frac{\mathrm{d}\xi_S}{\mathrm{d}\tau} = -\cos\tau \tag{A7}$$

and consideration of triangle NJL in Figure 9b shows that equation A5 must be replaced by

$$\frac{\mathrm{d}\sigma}{\mathrm{d}s} = \sin(\theta + \psi) \tag{A8}$$

Using the identity $\sin(\theta + \psi) = \sin\theta\cos\psi + \cos\theta\sin\psi$, and equations A2, A3, A4 and A8 we deduce that:

$$f_I(\tau; M) = \frac{1}{2\pi}\left[1 + \frac{\tan\psi}{M}\right], \quad \text{if} \quad \frac{\mathrm{d}\xi_S}{\mathrm{d}\tau} < 0 \tag{A9}$$

Equations A1, A6, A7 and A9, yield:

$$f_I(\tau; M) = \begin{cases} \frac{1}{2\pi}\left[1 - \frac{\cos\tau}{M}\right] & \text{if } \tau \in [\tau_1, \tau_2] \\ 0 & \text{otherwise} \end{cases} \tag{A10}$$

where the range of validity $[\tau_1, \tau_2]$ of the PDF has yet to be determined. Since $f_I(\tau, M)$ is a PDF it must be non-negative on $[\tau_1, \tau_2]$ and satisfy an integral constraint of the form

$$\int_{\tau_1}^{\tau_2} f_I(\tau; M)\mathrm{d}\tau = 1 \tag{A11}$$

The minimum and maximum initiation times τ_1 and τ_2 can now be derived as functions of M by considering the cases $M \geq 1$ and $M < 1$ separately.

Firstly, when $M \geq 1$, Figure 3a shows that all initiation times in the range $[0, 2\pi]$ are possible. Also, we note from equation A10 that

$$f_I(\tau; M) \geq 0, \forall\tau \in [0, 2\pi], \int_0^{2\pi} f_I(\tau; M)d\tau = 1 \tag{A12}$$

It follows that

$$\tau_1 = 0, \quad \tau_2 = 2\pi \quad \text{if } M \geq 1 \tag{A13}$$

We now consider the case when $M < 1$. Initiation events are now restricted to occur between time limits which are functions of M (Figure 3b). On geometrical grounds, we deduce that the maximum initiation time τ_2 is the value of τ in the range $[0, 2\pi]$ for which $\xi_S(\tau) \leq 0$ and for which a load line $\xi_L(\tau)$ is tangent to the strength curve $\xi_S(\tau)$. With the convention that the inverse cosine function $\cos^{-1}(M)$ returns a radian value in the range $[0, \pi]$, it follows that τ_2 satisfies:

$$\tau_2 = 2\pi - \cos^{-1}(M) \tag{A14}$$

Geometrical considerations (Figure 3*b*) show that the minimum initiation time τ_1 is the value of τ at which a load line tangent to the strength curve at $\tau_2 - 2\pi$ intersects the strength curve. Since the load line has slope M, this means that τ_1 satisfies

$$\sin\tau_1 = \sin(\tau_2 - 2\pi) + M(\tau_1 - (\tau_2 - 2\pi)) \qquad \text{(A15)}$$

Acknowledgments.
We thank P.E. Jupp for statistical advice. T.J. is supported by the Newton Trust, Cambridge. D.P. and B.M. are supported by the Natural Environment Research Council (UK).

References

Cox, D.R. and Lewis, P.A.W. (1966), *The Statistical Analysis of Series of Events*, Methuen, London.

Dzurisin (1980), Influence of fortnightly Earth tides at Kilauea volcano, *Geophys. Res. Lett.,* vol. 7, pp. 925 - 928.

Gao, S.G., Silver, P.G., Linde, A.T. and Sacks, I. S. (2000), Annual modulation of triggered seismicity following the 1992 Landers earthquake in California, *Nature*, vol. 406, pp. 500 - 504.

Glazner, A.F., Manley, C.R., Marron, J.S., Rojstaczer, S. (1999), Fire or ice: Anticorrelation of volcanism and glaciation in California over the past 800,000 years, *Geophys. Res. Lett.,* vol. 26, No. 12, pp. 1759-1762.

Heki, K. (2001), Seasonal modulation of interseismic strain buildup in Northeastern Japan driven by snow loads, *Science*, vol. 293, pp. 89 - 92.

Jammalamadaka, S.R. and Kozubowski, T.J. (2001), A wrapped exponential circular model, *Andhra Pradesh Academy of Sciences - a special issue in honor of C.R. Rao*, vol. 5, No.1, pp. 43 - 56.

Jeffreys, H. (1961), *Theory of Probability*, Clarendon Press, Oxford.

Johnston, M.J.S. and Mauk, F.J. (1972), Earth tides and the triggering of eruptions from Mt. Stromboli, Italy, *Nature*, vol. 239, pp. 266 - 267.

Jull, M., and McKenzie, D. (1996), The effect of deglaciation on mantle melting beneath Iceland, *J. Geophys. Res.,* vol. 101, No. B10, pp. 21815 - 21828.

Kalbfleisch, J.D. and Prentice, R.L. (1980), *The Statistical Analysis of Failure Time Data*, Wiley, New York.

Lockner, D.A. and Beeler, N.M. (1999), Premonitory slip and tidal triggering of earthquakes, *J. Geophys. Res.,* vol. 104, No. B9, pp. 20133 - 20151.

McNutt, S.R. and Beavan, R.J., (1987) Eruptions of Pavlof volcano and their possible modulation by ocean load and tectonic stresses, *J. Geophys. Res.,* vol. 92, No. B11, pp. 11509 - 11523.

Mardia, K.V. and Jupp, P.E. (2000), *Directional Statistics*, Wiley, Chichester.

Mauk, F.J. and Johnston, M.J.S. (1973), On the Triggering of Volcanic Eruptions by Earth Tides, *J. Geophys. Res.,* vol. 78, No. 17, pp. 3356 - 3375.

McGuire, W.J., Howarth R.J., Firth, C.R., Solow, A.R., Pullen, A.D., Saunders, S.J., Stewart, I.S. and Vita-Finzi, C. (1997), Correlation between rate of sea-level change and frequency of explosive volcanism in the Mediterranean, *Nature*, vol. 389, pp. 473 - 476.

Mason, B.G., Pyle D.M., Dade, W.B. and Jupp, T. (2002), Seasonality of volcanic eruptions, *submitted to J. Geophys. Res.,* 2002.

Mastin, L.G. (1994), Explosive tephra emissions at Mount St. Helens, 1989-1991 - the violent escape of magmatic gas following storms, *Geol. Soc. Am. Bull.*, vol. 106, No. 2, pp. 175 - 185.

Neuberg, J. (2000), External modulation of volcanic activity, *Geophys. J. Int.*, vol. 142, pp. 232 - 240.

Perfettini, H. and Schmittbuhl, J. (2001), Periodic loading on a creeping fault: implications for tides, *Geophys. Res. Lett.,* vol. 28, No. 3, pp. 435 - 438.

Sparks, R.S.J. (1981), Triggering of volcanic eruptions by earth tides , *Nature*, vol. 290, p. 448.

Stein, R.S. (1999), The role of stress transfer in earthquake occurrence, *Nature*, vol. 402, pp. 605 - 609.

Vidale, J.E., Agnew, D.C., Johnston, M.J.S. and Oppenheimer, D.H. (1998), Absence of earthquake correlation with Earth tides: An indication of high preseismic fault stress rate, *J. Geophys. Res.,* vol. 103, No. B10, pp. 24567 - 24572.

Wilcock, W.S.D. (2001), Tidal triggering of microearthquakes on the Juan de Fuca Ridge, *Geophys. Res. Lett.,* vol. 28, No. 20, pp. 3999 - 4002.

T. E. Jupp, BP Institute for Multiphase Flow, Madingley Rise, Madingley Road, Cambridge, CB3 0EZ, U.K.

D. M. Pyle and B. G. Mason, Department of Earth Sciences Downing Street, Cambridge, CB2 3EQ, U.K. (e-mail: tim@bpi.cam.ac.uk; dmp11@esc.cam.ac.uk; bgm21@hermes.cam.ac.uk; W.Brian.Dade@dartmouth.edu)

W. B. Dade, Department of Earth Sciences, Dartmouth College, Hanover, New Hamphsire, NH 03755, U.S.A.

(Received _____.)